Nonlinear Analysis: Modelling and Control, Vol. 23, No. 2, 213–233 ISSN 1392-5113
https://doi.org/10.15388/NA.2018.2.5

Pulsating flow of Casson fluid in a porous channel with thermal radiation, chemical reaction and applied magnetic field

Suripeddi Srinivas[a], **Challa Kalyan Kumar**[b], **Anala Subramanyam Reddy**[c]

[a]Department of Mathematics, VIT-AP (Deemed to be University),
Inavolu Village, Amaravati – 522237, India
srinivas.s@vitap.ac.in

[b]Department of Mathematics, Narayana Engineering College,
Gudur, SPSR Nellore – 524 101, India

[c]Department of Mathematics, School of Advanced Sciences,
Vellore Institute of Technology,
Vellore – 632 014, India

Received: May 22, 2017 / **Revised:** November 18, 2017 / **Published online:** February 12, 2018

Abstract. In the present analysis, the influence of thermal radiation, chemical reaction and thermal-diffusion on hydromagnetic pulsating flow of Casson fluid in a porous channel is investigated. The fluid is injected from the lower wall and sucked out from the upper wall with the same velocity. The governing flow equations are solved analytically by employing the perturbation technique. The influence of various emerging parameters on flow variables has been discussed. The obtained results show that the temperature distribution increases when there is an increase in heat source, whereas there is a decrease in temperature with an increase in radiation parameter. The concentration distribution decreases with an increase in chemical reaction parameter, while it increases for a given increase in Soret number. Further, the results reveal that, for both the Newtonian and non-Newtonian cases, Nusselt number distribution decreases at the upper wall with increasing Hartmann number and radiation parameter. The mass transfer rate decreases at the upper wall with increasing chemical reaction parameter and Soret number.

Keywords: pulsating flow, Casson fluid, porous channel, thermal radiation, Soret number, heat source/sink.

1 Introduction

Studies related to pulsating flow in a porous channel or pipe have attracted several researchers due to their applications in technological as well as biological flows such as transpiration cooling, gaseous diffusion, circulatory system and respiratory system, flow of blood, the process of dialysis of blood in an artificial kidney [18, 32, 41, 47]. Radhakrishnamacharya and Maiti [33] made an investigation of heat transfer to pulsatile flow in a porous channel. In their investigation, the fluid is injected through one wall

and sucked out through the opposite wall at the same rate. Bestman [7] discussed that a combined forced and free convection flow through an inclined porous channel when a pulsatile pressure is applied across its ends. Datta et al. [10] studied the unsteady heat transfer pulsatile flow of a dusty fluid in a porous channel by employing the perturbation technique. Vajravelu et al. [46] has analyzed the pulsatile flow of viscous fluid between two permeable beds. Shit and Roy [38] appraised the flow and heat transfer characteristics of pulsating flow of magneto-micropolar fluid through a stenosed artery.

In 1959, Casson first introduced Casson fluid to analyze the flow behaviour of pigment-oil of printing ink, which shows yield stress in constitutive equation. Based on rheological characteristics, the Casson fluid is classified as the most popular non-Newtonian fluid. The Casson fluid model can be chosen to analyze the rheological behaviour of ingredients like tomato sauce, soup, honey, jelly and human blood [9,21–23,26]. Since the blood contains several substances such as fibrinogen, protein, globulin in aqueous base plasma and human red blood cells, Casson fluid can be preferred to analyze the flow characteristics of blood. Sankar [36] studied the pulsatile flow of blood through a catheterized artery by considering blood as Casson fluid. Abolbashari et al. [1] analytically analyzed the flow, heat and mass transfer characteristics of Casson nanofluid flow over a stretching surface. Sivaraj and Benazir [40] studied the unsteady hydromagnetic mixed convection flow of Casson fluid in a porous asymmetric wavy channel.

Studies pertaining to magnetohydrodynamic flow of non-Newtonian fluid in a porous medium have gained much attention of many researchers due to its applications in the geothermal sources investigation, the optimization of solidification processes of metals and metal alloys, and nuclear fuel debris treatment [3, 11, 20, 29]. Ali et al. [3] analyzed the hydromagnetic effects on blood flow in a horizontal circular tube by considering blood as Casson fluid. Khan et al. [15] examined the unsteady squeezing hydromagnetic flow of a Casson fluid between parallel plates. Vajravelu et al. [45] studied the mixed convective flow of a Casson fluid over a vertical stretching sheet by using optimal homotopy analysis method. Rashidi et al. [34] investigated laminar-free convective flow of a two-dimensional electrically conducting viscoelastic fluid over a moving stretching surface in the presence of a porous medium. Attia and Sayed-Ahmed [4] analyzed the unsteady magnetohydrodynamic flow of Casson fluid between two parallel non-conducting porous plates. The transient squeezing flow of a magneto-micropolar biofluid in a noncompressible porous medium intercalated between two parallel plates in the presence of a uniform strength transverse magnetic field is investigated by Beg et al. [5]. The MHD boundary layer flow of a Casson fluid over an exponentially permeable shrinking sheet has been investigated by Nadeem et al. [25]. The problem of heat transfer to hydromagnetic pulsatile flow of Oldroyd fluid was studied by Srinivas et al. [42]. Prasad et al. [30] examined the flow and heat transfer of Casson nanofluid over a stretching sheet with variable thickness in the presence of a magnetic field.

Thermal radiation plays an imperative role in many engineering processes, which operate at high temperature such as gas turbines, nuclear plants and various propulsion devices. It is interesting to note that the thermal regulation in human blood flow by means of thermal radiation is most important in many medical treatments such as muscle spasm, chronic wide-spread pain, myalgia and thermal therapeutic [13, 17, 23, 39, 43]. Sinha

and Shit [39] investigated the problem of electromagnetohydrodynamic flow and transfer of blood in a capillary with thermal radiation. Palani and Abbas [27] explored the free convection MHD flow from a impulsively saturated vertical plate with thermal radiation. The effect of thermal radiation and viscous dissipation on a combined free and forced convective flow in a vertical channel is investigated by Prasad et al. [28]. Beg et al. [6] studied the combined heat and mass transfer by mixed magneto-convective flow of an electrically conducting flow along a moving radiating vertical flat plate with hydrodynamic slip and thermal convective boundary conditions. Mabood et al. [16] analyzed the influence of variable fluid properties on MHD flow of Casson fluid over a moving surface in the presence porous medium and radiation. Shehzad et al. [37] analytically studied the slip and thermal radiation effects on Casson fluid over a stretching surface by using homotopy analysis method.

The study related to heat and mass transfer with chemical reaction is of great practical importance in many engineering and industrial processes. Possible applications can be found in many industries like electric power industry, chemical industry and food processing chemical industry and so on. In many chemical engineering processes, a chemical reaction between a foreign mass and the fluid does occur. These processes occur in numerous industrial applications such as the polymer production, the manufacturing of ceramics or glassware, the food processing [8, 12, 23, 35, 44]. Afify and Elgazery [2] studied the chemical reaction effect on MHD stagnation point flow towards a stretching sheet with suction or injection. Mythili et al. [24] carried out a numerical study to analyse the chemical reaction, cross diffusion effects on Casson fluid over a cone and flat plate. Hayat et al. [14] discussed the chemical reaction, Soret and Dufour effects on peristaltic flow of Casson fluid in a two-dimensional asymmetric channel. Prasad et al. [31] studied the effects of applied magnetic field, thermal and species concentration on flow, heat and mass transfer of Casson fluid over a vertical permeable stretching sheet. Recently, Malathy et al. [19] examined the chemical reaction and thermal radiation effects on MHD pulsating flow of an Oldroyd-B fluid in channel with slip and convective boundary conditions.

The literature reveals that no study related to MHD pulsatile flow of Casson fluid in a porous channel with thermal radiation and chemical reaction has been explored so far. The main aim of the present investigation is to explore the influence of thermal radiation, chemical reaction, Soret and Joule's heating effects on MHD pulsating flow of Casson fluid in a porous channel with porous medium. The dimensionless governing flow equations are solved analytically by using perturbation technique. The influence of various parameters on flow variables has been discussed.

2 Mathematical formulation

Consider the pulsatile flow of an incompressible Casson fluid in a porous channel under the influence of uniform transverse applied magnetic field. The flow is driven by an unsteady pressure gradient [33],

$$-\frac{1}{\rho}\frac{\partial p^*}{\partial x^*} = A\big\{1 + \epsilon \exp(\mathrm{i}\omega t^*)\big\},$$

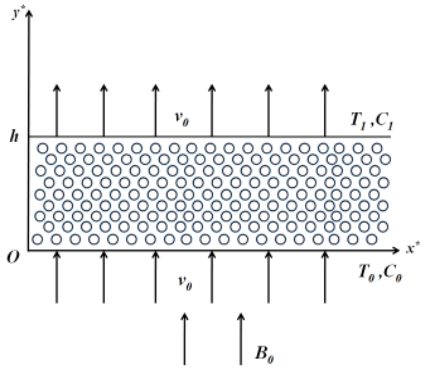

Figure 1. Schematic diagram of the model.

where ρ is density of the fluid, p^* is pressure, A is a known constant, $\epsilon \ll 1$ is a suitable chosen positive quantity, ω is the frequency and t^* is time. As shown in Fig. 1, a Cartesian coordinate system is taken in such a way that the x^*-axis is taken along lower wall and the y^*-axis perpendicular to it. The lower wall maintains temperature T_0 and a concentration C_0 and the upper wall maintains temperature T_1 ($T_1 > T_0$) and concentration C_1 ($C_1 > C_0$). A uniform magnetic field B_0 is imposed along the direction normal to the flow. The fluid is injected into the channel from the lower wall with a velocity v_0 and is sucked out through the upper wall with the same velocity. Rheological equation for Casson fluid is defined as follows [9, 21, 22, 26]:

$$\tau_{ij} = \begin{cases} (\mu_B + P_{y^*}/\sqrt{2\pi_c})2e_{ij}, & \pi_c > \pi, \\ (\mu_B + P_{y^*}/\sqrt{2\pi})2e_{ij}, & \pi > \pi_c, \end{cases}$$

where τ_{ij} is the (i,j)th component of the stress tensor, $\pi = e_{ij}e_{ij}$ with e_{ij} being the (i,j)th component of the deformation rate, π depicts the product of the component of the deformation rate with itself, π_c is the critical value of this product based on the non-Newtonian model, μ_B is the plastic dynamic viscosity of the non-Newtonian fluid, P_{y^*} is the yield stress of the fluid. The problem's governing equations as follows [9, 21, 22, 25, 26, 33, 41]:

$$\frac{\partial u^*}{\partial t^*} + v_0\frac{\partial u^*}{\partial y^*} = -\frac{1}{\rho}\frac{\partial p^*}{\partial x^*} + \nu\left(1+\frac{1}{\beta}\right)\frac{\partial^2 u^*}{\partial y^{*2}} - \frac{\sigma B_0^2}{\rho}u^* - \frac{\mu\Phi}{\rho k}u^*, \tag{1}$$

$$0 = -\frac{1}{\rho}\frac{\partial p^*}{\partial y^*}, \tag{2}$$

$$\frac{\partial T^*}{\partial t^*} + v_0\frac{\partial T^*}{\partial y^*} = \frac{\kappa}{\rho C_p}\frac{\partial^2 T^*}{\partial y^{*2}} + \frac{\mu}{\rho C_p}\left(1+\frac{1}{\beta}\right)\left(\frac{\partial u^*}{\partial y^*}\right)^2 + \frac{\sigma B_0^2}{\rho C_p}u^{*2} - \frac{1}{\rho C_p}\frac{\partial q_r}{\partial y^*} + \frac{Q_0}{\rho C_p}(T^* - T_0), \tag{3}$$

$$\frac{\partial C^*}{\partial t^*} + v_0 \frac{\partial C^*}{\partial y^*} = D \frac{\partial^2 C^*}{\partial y^{*2}} + \frac{D k_T}{T m} \frac{\partial^2 T^*}{\partial y^{*2}} - k_1 C^*. \tag{4}$$

The boundary conditions for the present analysis are

$$\begin{aligned} u^* = 0, \quad T^* = T_0, \quad C^* = C_0 \quad \text{at } y^* = 0, \\ u^* = 0, \quad T^* = T_1, \quad C^* = C_1 \quad \text{at } y^* = h, \end{aligned}$$

where u^* is dimensional velocity in x^* direction, Φ and k are the porosity and permeability of porous medium, μ is the dynamic viscosity, σ is electrical conductivity, $\beta = \mu_B \sqrt{2\pi_c}/P_{y^*}$ is the Casson fluid parameter, ν is the kinematic viscosity, C_p is the specific heat at constant pressure, Q_0 is the coefficient of heat source/sink, q_r is the radiative heat flux, κ is the thermal conductivity, k_1 is the first-order chemical reaction rate ($k_1 < 0$ for generative reaction, $k_1 > 0$ for destructive reaction, $k_1 = 0$ for no reaction), T_m is the mean temperature of the fluid, D is the coefficient of mass diffusivity, k_T is the thermal diffusion ratio, T^*, C^* are the temperature and concentration of the fluid. By using Rosseland approximation for radiative heat flux, q_r is defined as [13, 16, 17, 43]

$$q_r = -\frac{4\sigma^*}{3K^*} \frac{\partial T^{*4}}{\partial y^*}, \tag{5}$$

where K^* is the Rosseland mean absorption coefficient, σ^* is the Stefan–Boltzmann constant.

We presume that the temperature variation within the flow are sufficiently small such that T^{*4} may be expanded in a Taylor's series. Expanding T^{*4} about T_0 and neglecting higher-order terms we obtain

$$T^{*4} \cong 4T_0^3 T^* - 3T_0^4. \tag{6}$$

Substituting Eqs. (5) and (6) into Eq. (3), we obtain

$$\begin{aligned} \frac{\partial T^*}{\partial t^*} + v_0 \frac{\partial T^*}{\partial y^*} = {} & \frac{\kappa}{\rho C_p} \frac{\partial^2 T^*}{\partial y^{*2}} + \frac{\mu}{\rho C_p} \left(1 + \frac{1}{\beta}\right) \left(\frac{\partial u^*}{\partial y^*}\right)^2 + \frac{\sigma B_0^2}{\rho C_p} u^{*2} \\ & + \frac{1}{\rho C_p} \frac{16\sigma^* T_0^3}{3K^*} \frac{\partial^2 T^*}{\partial y^{*2}} + \frac{Q_0}{\rho C_p} (T^* - T_0). \end{aligned} \tag{7}$$

We introduce the following dimensionless variables [10, 33]:

$$\begin{aligned} x = \frac{x^*}{h}, \qquad y = \frac{y^*}{h}, \qquad t = t^* \omega, \qquad u = \frac{u^* \omega}{A}, \\ p = \frac{p^*}{\rho A h}, \qquad \theta = \frac{T^* - T_0}{T_1 - T_0}, \qquad \phi = \frac{C^* - C_0}{C_1 - C_0}. \end{aligned}$$

By using the above dimensionless variables, Eqs. (1), (7) and (4) become

$$H^2\frac{\partial u}{\partial t}+R\frac{\partial u}{\partial y}=-H^2\frac{\partial p}{\partial x}+\left(1+\frac{1}{\beta}\right)\left(\frac{\partial^2 u}{\partial y^2}\right)-\left(M^2+\frac{1}{Da}\right)u, \tag{8}$$

$$H^2\frac{\partial \theta}{\partial t}+R\frac{\partial \theta}{\partial y}=\frac{1}{Pr}\left(1+\frac{4}{3}Rd\right)\frac{\partial^2\theta}{\partial y^2}+\left(1+\frac{1}{\beta}\right)Ec\left(\frac{\partial u}{\partial y}\right)^2 + EcM^2u^2+Q\theta, \tag{9}$$

$$H^2\frac{\partial \phi}{\partial t}+R\frac{\partial \phi}{\partial y}=\frac{1}{Sc}\frac{\partial^2\phi}{\partial y^2}+Sr\frac{\partial^2\theta}{\partial y^2}-\gamma\phi-K_1, \tag{10}$$

where $Da=k/\Phi h^2$ is the Darcy number of the porous media, $M=B_0h\sqrt{\sigma}/\sqrt{\mu}$ is the Hartmann number, $H=h\sqrt{\omega}/\sqrt{\nu}$ is the frequency parameter, $R=v_0h/\nu$ is cross flow Reynolds number, $Q=Q_0h^2/(\rho C_p\nu)$ is heat source/sink parameter (i.e., positive for heat source and negative for heat sink), $Ec=(A/\omega)^2/(C_p(T_1-T_0))$ is the Eckert number, $Rd=4\sigma^*T_0^3/(\kappa K^*)$ is the radiation parameter, $Pr=\mu C_p/\kappa$ is the Prandtl number, $Sc=\nu/D$ is the Schmidt number, $Sr=DK_T(T_1-T_0)/(T_m\nu(C_1-C_0))$ is the Soret number, $\gamma=k_1h^2/\nu$ is the chemical reaction parameter, which is positive for destructive chemical reaction and negative for generative reaction and $K_1=k_1C_0h^2/(\nu(C_1-C_0))$.

So, the new boundary conditions are

$$\begin{aligned} &u=0, \quad \theta=0, \quad \phi=0 \quad \text{at } y=0,\\ &u=0, \quad \theta=1, \quad \phi=1 \quad \text{at } y=1. \end{aligned}$$

3 Method of solution

The velocity u, temperature θ and concentration ϕ can be assumed to have the form

$$u=u_0(y)+\varepsilon u_1(y)\exp(\mathrm{i}t)+\varepsilon^2u_2(y)\exp(2\mathrm{i}t), \tag{11}$$

$$\theta=\theta_0(y)+\varepsilon\theta_1(y)\exp(\mathrm{i}t)+\varepsilon^2\theta_2(y)\exp(2\mathrm{i}t), \tag{12}$$

$$\phi=\phi_0(y)+\varepsilon\phi_1(y)\exp(\mathrm{i}t)+\varepsilon^2\phi_2(y)\exp(2\mathrm{i}t). \tag{13}$$

Now substitute Eqs. (11)–(13) into Eqs. (8)–(10) and then equating the coefficients of various powers of ε, we get

$$\left(1+\frac{1}{\beta}\right)u_0''-Ru_0'-\left(M^2+\frac{1}{Da}\right)u_0+H^2=0, \tag{14}$$

$$\left(1+\frac{1}{\beta}\right)u_1''-Ru_1'-\left(M^2+\frac{1}{Da}+\mathrm{i}H^2\right)u_1+H^2=0, \tag{15}$$

$$\left(1+\frac{1}{\beta}\right)u_2''-Ru_2'-\left(M^2+\frac{1}{Da}+2\mathrm{i}H^2\right)u_2+H^2=0, \tag{16}$$

$$\left(1+\frac{4}{3}Rd\right)\theta_0''-PrR\theta_0'+\left(1+\frac{1}{\beta}\right)EcPru_0'^2+M^2EcPru_0^2+QPr\theta_0=0, \tag{17}$$

$$\left(1+\frac{4}{3}Rd\right)\theta_1'' - PrR\theta_1' - iH^2Pr\theta_1 + 2\left(1+\frac{1}{\beta}\right)EcPru_0'u_1' + 2M^2EcPru_0u_1 + QPr\theta_1 = 0, \tag{18}$$

$$\left(1+\frac{4}{3}Rd\right)\theta_2'' - PrR\theta_2' - 2iH^2Pr\theta_2 + \left(1+\frac{1}{\beta}\right)EcPru_1'^2 + M^2EcPru_1^2 + QPr\theta_2 = 0, \tag{19}$$

$$\phi_0'' - RSc\phi_0' - \gamma Sc\phi_0 + ScSr\theta_0'' - K_1Sc = 0, \tag{20}$$

$$\phi_1'' - RSc\phi_1' - \big(\mathrm{i}H^2Sc + \gamma Sc\big)\phi_1 + ScSr\theta_1'' = 0, \tag{21}$$

$$\phi_2'' - RSc\phi_2' - \big(2\mathrm{i}H^2Sc + \gamma Sc\big)\phi_2 + ScSr\theta_2'' = 0. \tag{22}$$

The corresponding boundary conditions are

$$\begin{array}{llllll} u_0(0)=0, & u_0(1)=0, & u_1(0)=0, & u_1(1)=0; & u_2(0)=0, & u_2(1)=0; \\ \theta_0(0)=0, & \theta_0(1)=1, & \theta_1(0)=0, & \theta_1(1)=0, & \theta_2(0)=0, & \theta_2(1)=0; \\ \phi_0(0)=0, & \phi_0(1)=1, & \phi_1(0)=0, & \phi_1(1)=0, & \phi_2(0)=0, & \phi_2(1)=0. \end{array} \tag{23}$$

By solving Eqs. (14)–(22) with the corresponding boundary conditions (23), we get

$$\begin{aligned} u_0 &= A_1\mathrm{e}^{m_1y} + A_2\mathrm{e}^{m_2y} + A_3, \\ u_1 &= A_4\mathrm{e}^{m_3y} + A_5\mathrm{e}^{m_4y} + A_6, \\ u_2 &= A_7\mathrm{e}^{m_5y} + A_8\mathrm{e}^{m_6y}, \end{aligned}$$

$$\begin{aligned} \theta_0 =& A_9\mathrm{e}^{m_7y} + A_{10}\mathrm{e}^{m_8y} + A_{11}\mathrm{e}^{2m_1y} + A_{12}\mathrm{e}^{2m_2y} + A_{13}\mathrm{e}^{m_1y} + A_{14}\mathrm{e}^{m_2y} \\ &+ A_{15}\mathrm{e}^{(m_1+m_2)y} + A_{16}, \\ \theta_1 =& A_{17}\mathrm{e}^{m_9y} + A_{18}\mathrm{e}^{m_{10}y} + A_{19}\mathrm{e}^{(m_1+m_3)y} + A_{20}\mathrm{e}^{(m_1+m_4)y} + A_{21}\mathrm{e}^{(m_2+m_3)y} \\ &+ A_{22}\mathrm{e}^{(m_2+m_4)y} + A_{23}\mathrm{e}^{m_1y} + A_{24}\mathrm{e}^{m_2y} + A_{25}\mathrm{e}^{m_3y} + A_{26}\mathrm{e}^{m_4y} + A_{27}, \\ \theta_2 =& A_{28}\mathrm{e}^{m_{11}y} + A_{29}\mathrm{e}^{m_{12}y} + A_{30}\mathrm{e}^{2m_3y} + A_{31}\mathrm{e}^{2m_4y} + A_{32}\mathrm{e}^{(m_3+m_4)y} \\ &+ A_{33}\mathrm{e}^{(m_1+m_3)y} + A_{34}\mathrm{e}^{(m_1+m_4)y} + A_{35}\mathrm{e}^{(m_2+m_3)y} + A_{36}\mathrm{e}^{(m_2+m_4)y} \\ &+ A_{37}\mathrm{e}^{(m_1+m_5)y} + A_{38}\mathrm{e}^{(m_1+m_6)y} + A_{39}\mathrm{e}^{(m_2+m_5)y} + A_{40}\mathrm{e}^{(m_2+m_6)y} \\ &+ A_{41}\mathrm{e}^{m_3y} + A_{42}\mathrm{e}^{m_4y} + A_{43}\mathrm{e}^{m_5y} + A_{44}\mathrm{e}^{m_6y} + A_{45}, \\ \phi_0 =& A_{46}\mathrm{e}^{m_{13}y} + A_{47}\mathrm{e}^{m_{14}y} + A_{48}\mathrm{e}^{m_7y} + A_{49}\mathrm{e}^{m_8y} + A_{50}\mathrm{e}^{2m_1y} + A_{51}\mathrm{e}^{2m_2y} \\ &+ A_{52}\mathrm{e}^{m_1y} + A_{53}\mathrm{e}^{m_2y} + A_{54}\mathrm{e}^{(m_1+m_2)y} + A_{55}, \\ \phi_1 =& A_{56}\mathrm{e}^{m_{15}y} + A_{57}\mathrm{e}^{m_{16}y} + A_{58}\mathrm{e}^{m_9y} + A_{59}\mathrm{e}^{m_{10}y} + A_{60}\mathrm{e}^{(m_1+m_3)y} \\ &+ A_{61}\mathrm{e}^{(m_1+m_4)y} + A_{62}\mathrm{e}^{(m_2+m_3)y} + A_{63}\mathrm{e}^{(m_2+m_4)y} + A_{64}\mathrm{e}^{m_1y} \\ &+ A_{65}\mathrm{e}^{m_2y} + A_{66}\mathrm{e}^{m_3y} + A_{67}\mathrm{e}^{m_4y}, \end{aligned}$$

$$\begin{aligned}\phi_2 =&A_{68}\mathrm{e}^{m_{17}y} + A_{69}\mathrm{e}^{m_{18}y} + A_{70}\mathrm{e}^{m_{11}y} + A_{71}\mathrm{e}^{m_{12}y} + A_{72}\mathrm{e}^{2m_3y} + A_{73}\mathrm{e}^{2m_4y}\\ &+ A_{74}\mathrm{e}^{(m_3+m_4)y} + A_{75}\mathrm{e}^{(m_1+m_3)y} + A_{76}\mathrm{e}^{(m_1+m_4)y} + A_{77}\mathrm{e}^{(m_2+m_3)y}\\ &+ A_{78}\mathrm{e}^{(m_2+m_4)y} + A_{79}\mathrm{e}^{(m_1+m_5)y} + A_{80}\mathrm{e}^{(m_1+m_6)y} + A_{81}\mathrm{e}^{(m_2+m_5)y}\\ &+ A_{82}\mathrm{e}^{(m_2+m_6)y} + A_{83}\mathrm{e}^{m_3y} + A_{84}\mathrm{e}^{m_4y} + A_{85}\mathrm{e}^{m_5y} + A_{86}\mathrm{e}^{m_6y},\end{aligned}$$

where m's and A's are constants given in Appendix.

Further, the dimensionless Nusselt and Sherwood numbers at the walls are given by $Nu = -(\partial\theta/\partial y)_{y=0,1} = -(\theta_0' + \varepsilon\theta_1'\mathrm{e}^{it} + \varepsilon^2\theta_2'\mathrm{e}^{2it})_{y=0,1}$ and $Sh = -(\partial\phi/\partial y)_{y=0,1} = -(\phi_0' + \varepsilon\phi_1'\mathrm{e}^{it} + \varepsilon^2\phi_2'\mathrm{e}^{2it})_{y=0,1}$.

4 Results and discussion

This section describes the influence of various physical parameters on the non-dimensional velocity, temperature, concentration, Nusselt number and sherwood number distributions graphically in Figs. 2–13.

In the present analysis, θ_s, ϕ_s,u_t, θ_t, ϕ_t represent steady temperature, steady concentration, unsteady velocity, unsteady temperature, unsteady concentration, respectively. Figure 2 presents the effects of Casson fluid parameter (β), Darcy number (Da), frequency parameter (H), Hartmann number (M) on the velocity distribution. From Figs. 2(a) and 2(c), it is notice that the velocity increases with an increase in Casson fluid parameter and frequency parameter. Figure 2(b) elucidates the variation of velocity for different values of Darcy number. It is noticed that the velocity is an increasing function of Da. Because the linear porous drag force, called the Darcian drag force, is inversely proportional to Darcy number (see the last term of Eq. (8), i.e., $-u/Da$). An increase in permeability of porous regions, will increase Da, which will act as the Darcian drag force. Hence, there is an increase in u with increase in Da. Figure 2(d) shows that for a given increase in M, there is a decrease in velocity. This is due to fact that the retarding forces (called Lorentz forces) generated by the applied magnetic field act as resistive drag forces opposite to the flow direction, which results a decrease in velocity. The effect of t on unsteady velocity distribution is shown in Fig. 3. One can noticed that the unsteady velocity profiles oscillate with increasing t.

Figures 4(a) and 4(b) shows the influence of the cross flow Reynolds number R and heat source/sink parameter Q on the temperature distribution. Figure 4(a) depicts that the temperature distribution decreases with an increase of R. From Fig. 4(b) one can observed that there is a rise in temperature with an increase of heat source, while it is decreases with an increase of heat sink. The effects of radiation parameter (Rd) Hartmann number (M) and Eckert number (Ec) on steady and unsteady temperature distributions are shown in Figs. 5–7. Figure 5 describes the variation of steady and unsteady temperature profiles for different values of radiation parameter. It is noticed that the steady temperature decreases for a given increase in radiation parameter (see Fig. 5(a)). From Fig. 5(b) one can see that the unsteady temperature oscillating with increasing Rd and the maximum is shifted to the near the walls. From Fig. 6(a) it is clear that the steady temperature decreases for

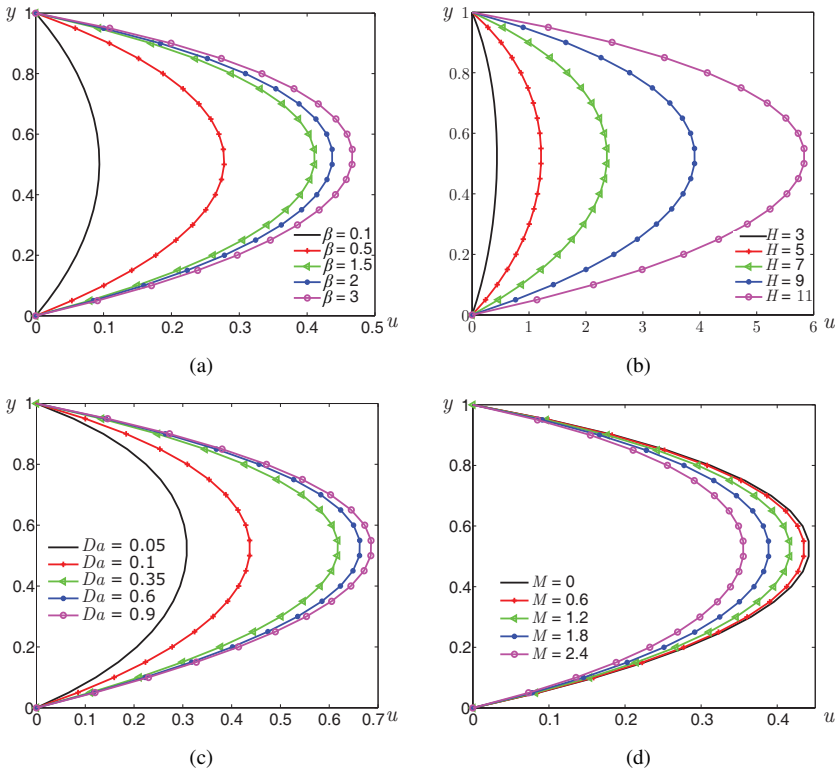

Figure 2. Velocity distribution for $\varepsilon = 0.01$, $t = \pi/4$, $R = 1$: (a) effect of β when $Da = 0.1$, $H = 3$, $M = 0.5$; (b) effect of H when $\beta = 2$, $Da = 0.1$, $M = 0.5$; (c) effect of Da when $\beta = 2$, $H = 3$, $M = 0.5$; (d) effect of M when $\beta = 2$, $Da = 0.1$, $H = 3$.

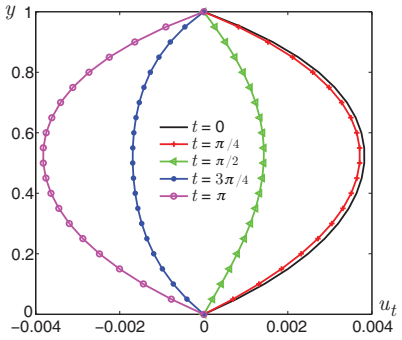

Figure 3. Effect of t on unsteady velocity distribution when $\varepsilon = 0.01$, $\beta = 2$, $H = 3$, $R = 1$, $M = 0.5$, $Da = 0.1$.

given increase in M towards the lower wall, while it increases towards the upper wall. From Fig. 6(b) one can infer that the unsteady temperature oscillates with increase M.

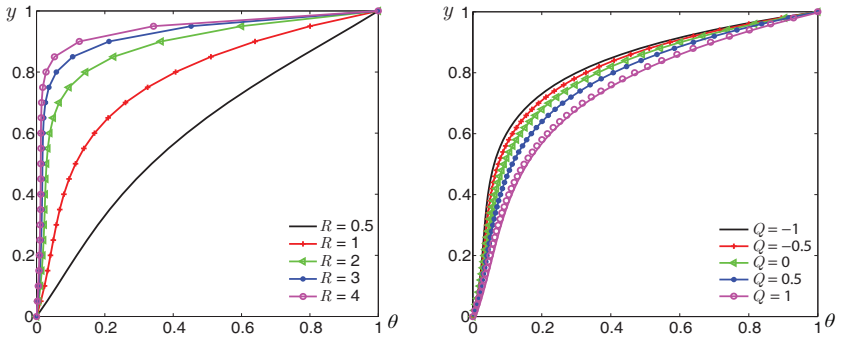

(a) (b)

Figure 4. Temperature distribution for $\varepsilon = 0.01$, $\beta = 2$, $M = 0.5$, $t = \pi/4$, $H = 3$, $Ec = 0.1$, $Pr = 21$, $Da = 0.1$, $Rd = 2$: (a) effect of R when $Q = 0.5$; (b) effect of Q when $R = 1$.

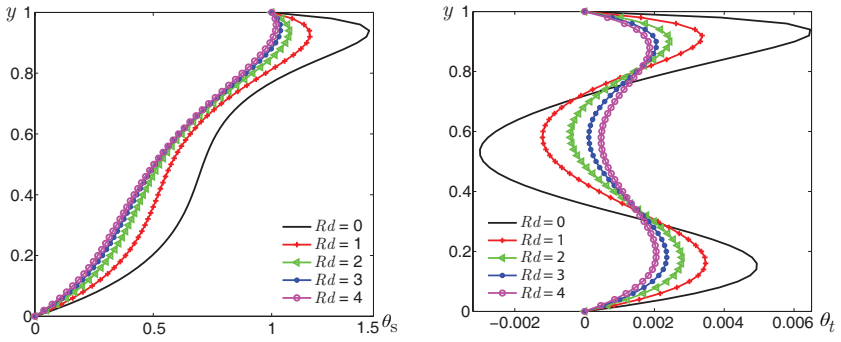

(a) (b)

Figure 5. Effect of Rd on temperature distribution when $\varepsilon = 0.01$, $\beta = 2$, $t = \pi/4$, $H = 3$, $M = 0.5$, $Pr = 21$, $Ec = 1$, $Da = 0.1$, $R = 1$, $Q = 0.5$.

Figure 7 presents the effect of Eckert number on steady and unsteady temperature distributions. From Fig. 7(a) one can noticed that the steady temperature increases with increasing Ec. This increase in temperature may be due to heat created by viscous distribution. From Fig. 7(b) it is observed that the unsteady temperature exhibits oscillating character with increasing Ec and the maximum is shifted to the boundary layers near the walls. The influence of time on unsteady temperature distribution is shown in Fig. 8. It is observed that the unsteady temperature profiles oscillate with increasing t.

Figures 9–11 show the effects of the chemical reaction parameter (γ), Schmidt number (Sc) and Soret number on steady and unsteady concentration distribution ϕ. Figure 9 depicts the influence of γ on steady and unsteady concentration distributions. It is observed that the steady and unsteady concentration distributions decrease with an increase of destructive chemical reaction ($\gamma > 0$). This is due to fact that increasing destructive chemical reaction there is a decrease in the concentration boundary layer because the destructive chemical reaction reduces the solutal boundary layer thickness

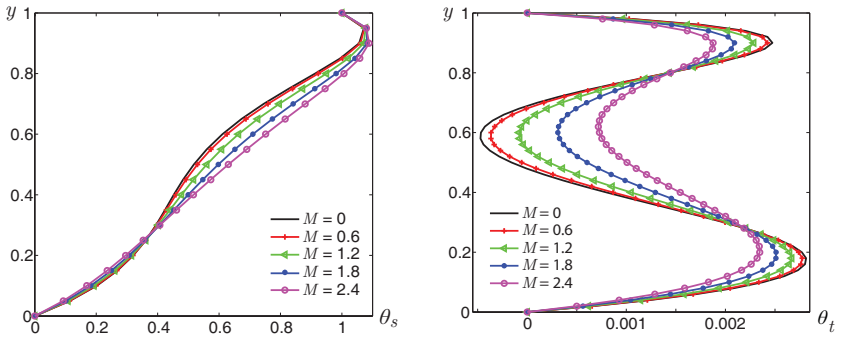

(a) (b)

Figure 6. Effect of M on temperature distribution when $\varepsilon = 0.01$, $\beta = 2$, $t = \pi/4$, $H = 3$, $Ec = 1$, $Pr = 21$, $Rd = 2$, $Da = 0.1$, $R = 1$, $Q = 0.5$.

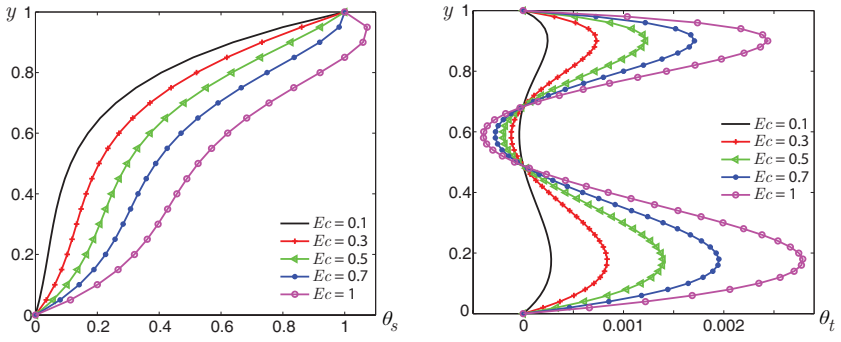

(a) (b)

Figure 7. Effect of Ec on temperature distribution when $\varepsilon = 0.01$, $\beta = 2$, $t = \pi/4$, $H = 3$, $M = 0.5$, $Pr = 21$, $Rd = 2$, $Da = 0.1$, $R = 1$, $Q = 0.5$.

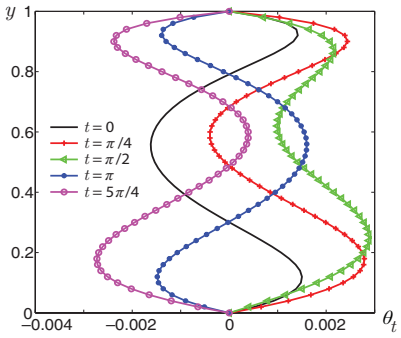

Figure 8. Effect of t on unsteady temperature distribution when $\varepsilon = 0.01$, $\beta = 2$, $Ec = 1$, $H = 3$, $M = 0.5$, $Pr = 21$, $Rd = 2$, $Da = 0.1$, $R = 1$, $Q = 0.5$.

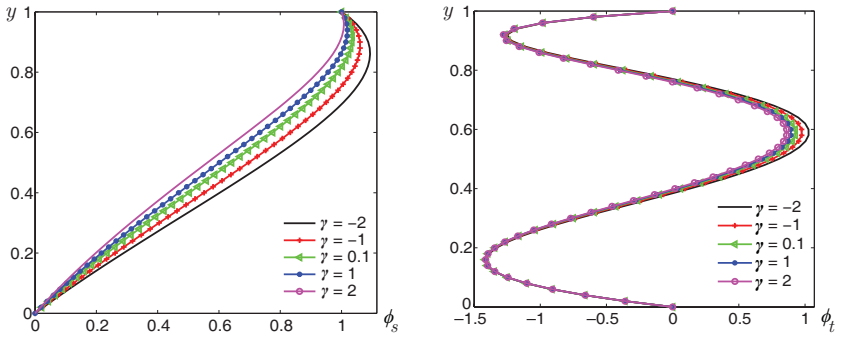

(a) (b)

Figure 9. Effect of γ on concentration distribution when $\varepsilon = 0.01$, $\beta = 2$, $Ec = 0.1$, $H = 3$, $t = \pi/4$, $M = 0.5$, $Pr = 21$, $Rd = 2$, $Da = 0.1$, $R = 1$, $Q = 0.5$, $K_1 = 0.001$, $Sc = 0.62$, $Sr = 1$.

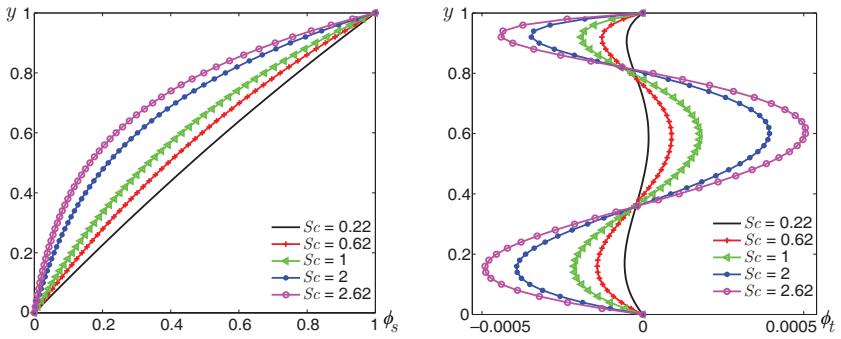

(a) (b)

Figure 10. Effect of Sc on concentration distribution when $\varepsilon = 0.01$, $\beta = 2$, $Ec = 0.1$, $H = 3$, $M = 0.5$, $t = \pi/4$, $Pr = 21$, $Rd = 2$, $Da = 0.1$, $R = 1$, $Q = 0.5$, $K_1 = 0.001$, $\gamma = 1$, $Sr = 1$.

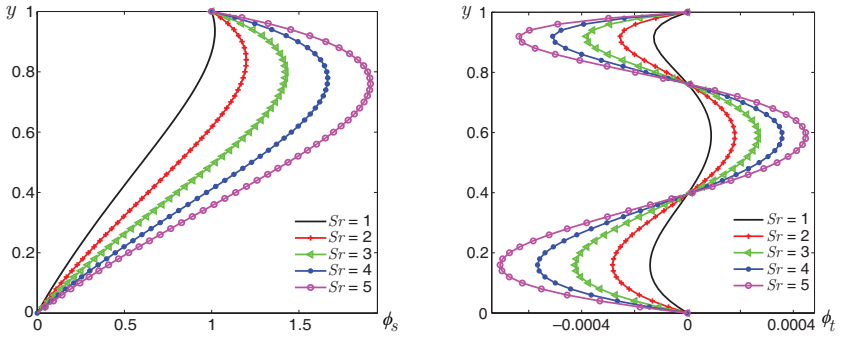

(a) (b)

Figure 11. Effect of Sr on concentration distribution when $\varepsilon = 0.01$, $\beta = 2$, $Ec = 0.1$, $H = 3$, $M = 0.5$, $t = \pi/4$, $Pr = 21$, $Rd = 2$, $Da = 0.1$, $R = 1$, $Q = 0.5$, $K_1 = 0.001$, $\gamma = 1$, $Sc = 0.62$.

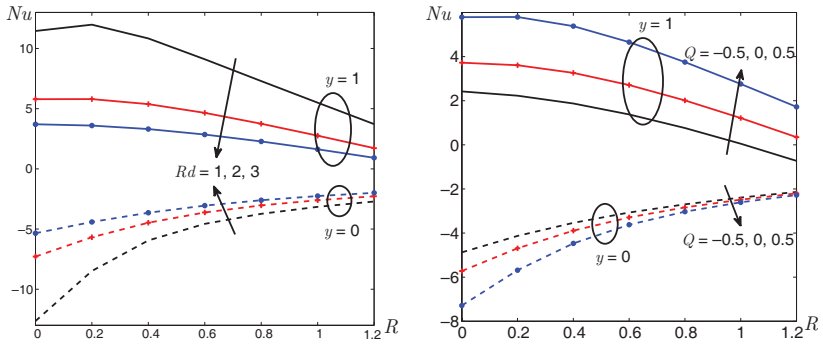

(a) (b)

Figure 12. Nusselt number distribution for $\varepsilon = 0.01$, $\beta = 2$, $M = 0.5$, $t = \pi/4$, $H = 3$, $Ec = 1$, $Pr = 21$, $Da = 0.1$: (a) effect of Rd when $Q = 0.5$; (b) effect of Q when $Rd = 2$.

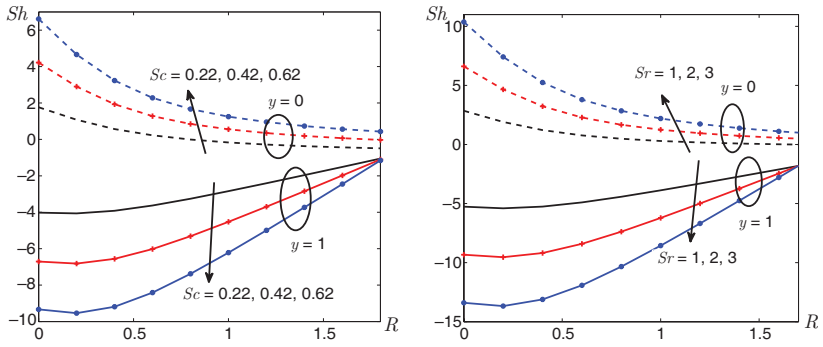

(a) (b)

Figure 13. Sherwood number distribution for $\varepsilon = 0.01$, $\beta = 2$, $M = 0.5$, $t = \pi/4$, $H = 3$, $Q = 0.5$, $Ec = 1$, $Da = 0.1$, $K_1 = 0.001$, $\gamma = 1$: (a) effect of Sc when $Sr = 2$; (b) effect of Sr when $Sc = 0.62$.

and increases the mass transfer. Further, the unsteady concentration exhibits oscillating character. The opposite behaviour can be observed for the case of generative chemical reaction. Figure 10(a) shows that the steady concentration distribution decreases for given increase in Sc. From Fig. 10(b) one can see that the unsteady concentration profiles exhibits oscillation character. From Fig. 11(a), it is seen that there is a rise in steady concentration with an increase of Sr. Figure 11(b) presents the oscillating character of unsteady concentration distribution by varying Sr.

Figure 12 elucidates the effects of Rd and Q on Nusselt number distribution (Nu) against R. From Fig. 12(a) it is noticed that for a given increase in Radiation parameter, Nu increases at the lower wall, while it decreases at the upper wall. From Fig. 12(b) one can infer that, at the upper wall Nu increases with increasing heat source, while it decreases at the lower wall. The behaviour is reversed for the case of heat sink. The effects of Sc and Sr on Sherwood number distribution (Sh) against R is shown in Fig. 13. From Fig. 13(a), one can be noticed that Sh is an increasing function of Sc at the lower wall,

Table 1. Comparison of Nusselt number for Newtonian and non-Newtonian cases when $\varepsilon = 0.01$, $t = \pi/4$, $H = 3$, $Ec = 1$, $Pr = 21$, $Da = 0.1$.

Parameter	Values	$Nu = -(\partial\theta/\partial y)_{y=0}$		$Nu = -(\partial\theta/\partial y)_{y=1}$	
		Newtonian	Non-Newtonian	Newtonian	Non-Newtonian
M	0	-2.7033	-2.6361	3.1771	2.7457
	2	-2.2726	-2.2307	3.5754	2.7261
	4	-1.5615	-1.5380	2.6740	1.8116
R	0	-7.6829	-7.1678	6.1846	5.6695
	1	-2.2726	-2.2307	3.5754	2.7261
	2	-1.1585	-1.2067	-1.9577	-2.8056
Q	0	-2.5506	-2.4868	1.6763	1.2142
	0.5	-2.6712	-2.6064	3.2306	2.7556
	1	-2.8333	-2.7671	5.4356	4.9425
Rd	0	-4.2702	-4.1034	19.2777	17.4188
	1	-3.3850	-3.2904	6.2590	5.4984
	2	-2.8333	-2.7671	3.2306	2.7556

Table 2. Comparison of Sherwood number for Newtonian and non-Newtonian cases when $\varepsilon = 0.01$, $M = 0.5$, $t = \pi/4$, $H = 3$, $Q = 0.5$, $Ec = 1$, $Da = 0.1$, $K_1 = 0.001$, $Rd = 2$.

Parameter	Values	$Sh = -(\partial\phi/\partial y)_{y=0}$		$Sh = -(\partial\phi/\partial y)_{y=1}$	
		Newtonian	Non-Newtonian	Newtonian	Non-Newtonian
Sc	0.22	-0.3248	-0.3373	-3.2051	-2.8299
	0.62	0.7586	0.7495	-7.2520	-6.1884
	1	1.6468	1.6638	-11.1336	-9.4111
	2	3.5253	3.6642	-21.4679	-18.0043
γ	0	-0.3507	-0.3646	-3.1424	-2.7645
	0.5	-0.3376	-0.3508	-3.2051	-2.7974
	1.5	-0.3124	-0.3241	-3.2357	-2.8619
Sr	0	-0.8620	-0.8620	-1.1863	-1.1863
	1	-0.5934	-0.5996	-2.1957	-2.0081
	2	-0.3248	-0.3373	-3.2051	-2.8299

while it is a decreasing function at the upper wall. From Fig. 13(b), the similar behaviour can be observed by varying Sr.

Tables 1 and 2 show the variations of Nu and Sh for both the Newtonian and non-Newtonian cases. From Table 1 it is observed that for both the Newtonian and non-Newtonian cases, the Nusselt number distribution decreases at the upper wall with increasing M, R and Rd, while it decreases with increasing Q. However, this behaviour is reversed at lower wall. Table 2 depicts that the Sherwood number distribution is an increasing function of Sc, γ, and Sr for both the Newtonian and non-Newtonian cases at lower wall, while it is decreasing function at upper wall.

5 Conclusion

The present study deals with hydromagnetic pulsating flow of Casson fluid in a porous channel with thermal radiation and chemical reaction in the presence of heat source/sink. The problem considered is important as flow of Casson fluids (blood, drilling muds,

clay coating, certain oils, greases and many impulsions) in porous channel are used in modelling biological and industrial research. The governing flow equations are solved analytically by employing perturbation technique. The main findings of the present study are given below:

- The velocity distribution increases with increasing Casson fluid parameter, frequency parameter and Darcy number, while it decreases with increasing Hartmann number.
- The temperature increases with increasing heat source whereas it decreases with increasing heat sink.
- The steady temperature distribution is an increasing function of Ec, while it is a decreasing function of Rd.
- The concentration distribution decreases with increasing destructive chemical reaction and Schmidt number, while it increases with increasing Soret number.
- Nusselt number at upper wall increases with increasing heat source, while it decreases with increasing Rd. But this behaviour is reversed at the lower wall.
- Sherwood number at lower wall is a increasing function of Sc and Sr whereas it is a decreasing function at the upper wall.
- By taking $M = 0$, as a limiting case, the results corresponding to the problem for the hydrodynamic case can be captured.
- The results of Radhakrishnamacharya and Maiti [33] (i.e., for the case of Newtonian fluid) can be captured from the present analysis by taking $\beta \to \infty$, $M = Q = Rd = \gamma = Sr = Sc = 0$ in the absence of mass (concentration) diffusion.

Appendix

$$m_{1,2} = \frac{R \pm \sqrt{R^2 + 4B_1B_2}}{2B_1}; \quad B_1 = 1 + \frac{1}{\beta}; \quad B_2 = M^2 + \frac{1}{Da}; \quad A_3 = \frac{H^2}{B_2};$$

$$A_1 = \frac{A_3(\mathrm{e}^{m_1} - 1)}{\mathrm{e}^{m_1} - \mathrm{e}^{m_2}} - A_3; \quad A_2 = -\frac{A_3(\mathrm{e}^{m_1} - 1)}{\mathrm{e}^{m_1} - \mathrm{e}^{m_2}}; \quad B_3 = M^2 + \frac{1}{Da} + \mathrm{i}H^2;$$

$$m_{3,4} = \frac{R \pm \sqrt{R^2 + 4B_1B_3}}{2B_1}; \quad A_6 = \frac{H^2}{B_3}; \quad A_5 = -\frac{A_6(\mathrm{e}^{m_3} - 1)}{\mathrm{e}^{m_3} - \mathrm{e}^{m_4}}; \quad A_4 = \frac{A_6(\mathrm{e}^{m_3} - 1)}{\mathrm{e}^{m_3} - \mathrm{e}^{m_4}} - A_6;$$

$$m_{5,6} = \frac{R \pm \sqrt{R^2 + 4B_1B_4}}{2B_1}; \quad B_4 = M^2 + \frac{1}{Da} + 2\mathrm{i}H^2; \quad A_7 = 0; \quad A_8 = 0;$$

$$B_5 = 1 + \frac{4}{3}Rd; \quad B_6 = PrR; \quad B_7 = QPr;$$

$$m_{7,8} = \frac{B_6 \pm \sqrt{B_6^2 - 4B_5B_7}}{2B_5}; \quad B_8 = \left(1 + \frac{1}{\beta}\right)EcPr; \quad B_9 = M^2EcPr;$$

$$A_{11} = -\frac{B_8m_1^2A_1^2 + B_9A_1^2}{4m_1^2B_5 - 2m_1B_6 + B_7}; \quad A_{12} = -\frac{B_8m_2^2A_2^2 + B_9A_2^2}{4m_2^2B_5 - 2m_2B_6 + B_7};$$

$$A_{13} = -\frac{2B_9A_1A_3}{B_5m_1^2 - B_6m_1 + B_7}; \quad A_{14} = -\frac{2B_9A_2A_3}{B_5m_2^2 - B_6m_2 + B_7};$$

$$A_{15} = -\frac{2B_8 m_1 m_2 A_1 A_2 + 2B_9 A_1 A_2}{B_5(m_1+m_2)^2 - B_6(m_1+m_2) + B_7}; \quad A_{16} = -\frac{B_9 A_3^2}{B_7};$$

$$A_9 = -(A_{10} + A_{11} + A_{12} + A_{13} + A_{14} + A_{15} + A_{16});$$

$$A_{10} = \frac{1}{-\mathrm{e}^{m_7} + \mathrm{e}^{m_8}}\big(1 + A_{11}\big(\mathrm{e}^{m_7} - \mathrm{e}^{2m_1}\big) + A_{12}\big(\mathrm{e}^{m_7} - \mathrm{e}^{2m_2}\big) + A_{13}\big(\mathrm{e}^{m_7} - \mathrm{e}^{m_1}\big) + A_{14}\big(\mathrm{e}^{m_7} - \mathrm{e}^{m_2}\big) + A_{15}\big(\mathrm{e}^{m_7} - \mathrm{e}^{(m_1+m_2)}\big) + A_{16}\big(\mathrm{e}^{m_7} - 1\big)\big);$$

$$m_{9,10} = \frac{B_6 \pm \sqrt{B_6^2 - 4B_5 B_{10}}}{2B_5}; \quad B_{10} = QPr - \mathrm{i}H^2 Pr;$$

$$A_{19} = -\frac{2B_8 m_1 m_3 A_1 A_4 + 2B_9 A_1 A_4}{B_5(m_1+m_3)^2 - B_6(m_1+m_3) + B_{10}}; \quad A_{20} = -\frac{2B_8 m_1 m_4 A_1 A_5 + 2B_9 A_1 A_5}{B_5(m_1+m_4)^2 - B_6(m_1+m_4) + B_{10}};$$

$$A_{21} = -\frac{2B_8 m_2 m_3 A_2 A_4 + 2B_9 A_2 A_4}{B_5(m_2+m_3)^2 - B_6(m_2+m_3) + B_{10}}; \quad A_{22} = -\frac{2B_8 m_2 m_4 A_2 A_5 + 2B_9 A_2 A_5}{B_5(m_2+m_4)^2 - B_6(m_2+m_4) + B_{10}};$$

$$A_{23} = -\frac{2B_9 A_1 A_6}{B_5 m_1^2 - B_6 m_1 + B_{10}}; \quad A_{24} = -\frac{2B_9 A_2 A_6}{B_5 m_2^2 - B_6 m_2 + B_{10}};$$

$$A_{25} = -\frac{2B_9 A_3 A_4}{B_5 m_3^2 - B_6 m_3 + B_{10}}; \quad A_{26} = -\frac{2B_9 A_3 A_5}{B_5 m_4^2 - B_6 m_4 + B_{10}}; \quad A_{27} = -\frac{2B_9 A_3 A_6}{B_{10}};$$

$$A_{17} = -(A_{18} + A_{19} + A_{20} + A_{21} + A_{22} + A_{23} + A_{24} + A_{25} + A_{26} + A_{27});$$

$$A_{18} = \frac{1}{-\mathrm{e}^{m_9} + \mathrm{e}^{m_{10}}}\big(A_{19}\big(\mathrm{e}^{m_9} - \mathrm{e}^{(m_1+m_3)}\big) + A_{20}\big(\mathrm{e}^{m_9} - \mathrm{e}^{(m_1+m_4)}\big) + A_{21}\big(\mathrm{e}^{m_9} - \mathrm{e}^{(m_2+m_3)}\big) + A_{22}\big(\mathrm{e}^{m_9} - \mathrm{e}^{(m_2+m_4)}\big) + A_{23}\big(\mathrm{e}^{m_9} - \mathrm{e}^{m_1}\big) + A_{24}\big(\mathrm{e}^{m_9} - \mathrm{e}^{m_2}\big) + A_{25}\big(\mathrm{e}^{m_9} - \mathrm{e}^{m_3}\big) + A_{26}\big(\mathrm{e}^{m_9} - \mathrm{e}^{m_4}\big) + A_{27}\big(\mathrm{e}^{m_9} - 1\big)\big);$$

$$m_{11,12} = \frac{B_6 \pm \sqrt{B_6^2 - 4B_5 B_{11}}}{2B_5}; \quad B_{11} = QPr - 2\mathrm{i}H^2 Pr; \quad A_{30} = -\frac{B_8 A_4^2 m_3^2 + B_9 A_4^2}{4B_5 m_3^2 - 2B_6 m_3 + B_{11}};$$

$$A_{31} = -\frac{B_8 A_5^2 m_4^2 + B_9 A_5^2}{4B_5 m_4^2 - 2B_6 m_4 + B_{11}}; \quad A_{32} = -\frac{2B_8 m_3 m_4 A_4 A_5 + 2B_9 A_4 A_5}{B_5(m_3+m_4)^2 - B_6(m_3+m_4) + B_{11}};$$

$$A_{33} = -\frac{2B_8 m_1 m_3 A_1 A_4}{B_5(m_1+m_3)^2 - B_6(m_1+m_3) + B_{11}}; \quad A_{34} = -\frac{2B_8 m_1 m_4 A_1 A_5}{B_5(m_1+m_4)^2 - B_6(m_1+m_4) + B_{11}};$$

$$A_{35} = -\frac{2B_8 m_2 m_3 A_2 A_4}{B_5(m_2+m_3)^2 - B_6(m_2+m_3) + B_{11}}; \quad A_{36} = -\frac{2B_8 m_2 m_4 A_2 A_5}{B_5(m_2+m_4)^2 - B_6(m_2+m_4) + B_{11}};$$

$$A_{37} = -\frac{2B_9 A_1 A_7}{B_5(m_1+m_5)^2 - B_6(m_1+m_5) + B_{11}}; \quad A_{38} = -\frac{2B_9 A_1 A_8}{B_5(m_1+m_6)^2 - B_6(m_1+m_6) + B_{11}};$$

$$A_{39} = -\frac{2B_9 A_2 A_7}{B_5(m_2+m_5)^2 - B_6(m_2+m_5) + B_{11}}; \quad A_{40} = -\frac{2B_9 A_2 A_8}{B_5(m_2+m_6)^2 - B_6(m_2+m_6) + B_{11}};$$

$$A_{41} = -\frac{2B_9 A_4 A_6}{B_5 m_3^2 - B_6 m_3 + B_{11}}; \quad A_{42} = -\frac{2B_9 A_5 A_6}{B_5 m_4^2 - B_6 m_4 + B_{11}};$$

$$A_{43} = -\frac{2B_9 A_3 A_7}{B_5 m_5^2 - B_6 m_5 + B_{11}}; \quad A_{44} = -\frac{2B_9 A_3 A_8}{B_5 m_6^2 - B_6 m_6 + B_{11}}; \quad A_{45} = -\frac{B_9 A_6^2}{B_{11}};$$

$$A_{28} = -(A_{29} + A_{30} + A_{31} + A_{32} + A_{33} + A_{34} + A_{35} + A_{36} + A_{37} + A_{38} + A_{39} + A_{40} + A_{41} + A_{42} + A_{43} + A_{44} + A_{45});$$

$$A_{29} = \frac{1}{-\mathrm{e}^{m_{11}} + \mathrm{e}^{m_{12}}}\big(A_{30}\big(\mathrm{e}^{m_{11}} - \mathrm{e}^{2m_3}\big) + A_{31}\big(\mathrm{e}^{m_{11}} - \mathrm{e}^{2m_4}\big) + A_{32}\big(\mathrm{e}^{m_{11}} - \mathrm{e}^{(m_3+m_4)}\big) + A_{33}\big(\mathrm{e}^{m_{11}} - \mathrm{e}^{(m_1+m_3)}\big) + A_{34}\big(\mathrm{e}^{m_{11}} - \mathrm{e}^{(m_1+m_4)}\big) + A_{35}\big(\mathrm{e}^{m_{11}} - \mathrm{e}^{(m_2+m_3)}\big)$$

$$+ A_{36}\big(\mathrm{e}^{m_{11}} - \mathrm{e}^{(m_2+m_4)}\big) + A_{37}\big(\mathrm{e}^{m_{11}} - \mathrm{e}^{(m_1+m_5)}\big) + A_{38}\big(\mathrm{e}^{m_{11}} - \mathrm{e}^{(m_1+m_6)}\big)$$
$$+ A_{39}\big(\mathrm{e}^{m_{11}} - \mathrm{e}^{(m_2+m_5)}\big) + A_{40}\big(\mathrm{e}^{m_{11}} - \mathrm{e}^{(m_2+m_6)}\big) + A_{41}\big(\mathrm{e}^{m_{11}} - \mathrm{e}^{m_3}\big)$$
$$+ A_{42}\big(\mathrm{e}^{m_{11}} - \mathrm{e}^{m_4}\big) + A_{43}\big(\mathrm{e}^{m_{11}} - \mathrm{e}^{m_5}\big) + A_{44}\big(\mathrm{e}^{m_{11}} - \mathrm{e}^{m_6}\big) + A_{45}\big(\mathrm{e}^{m_{11}} - 1\big)\big);$$

$$m_{13,14} = \frac{B_{12} \pm \sqrt{B_{12}^2 + 4B_{13}}}{2}; \quad B_{12} = RSc; \quad B_{13} = \gamma Sc;$$

$$A_{48} = -\frac{ScSrA_9 m_7^2}{m_7^2 - B_{12}m_7 - B_{13}}; \quad A_{49} = -\frac{ScSrA_{10} m_8^2}{m_8^2 - B_{12}m_8 - B_{13}};$$

$$A_{50} = -\frac{4ScSrm_1^2 A_{11}}{4m_1^2 - 2m_1 B_{12} - B_{13}}; \quad A_{51} = -\frac{4ScSrm_2^2 A_{12}}{4m_2^2 - 2m_2 B_{12} - B_{13}};$$

$$A_{52} = -\frac{ScSrA_{13} m_1^2}{m_1^2 - B_{12}m_1 - B_{13}}; \quad A_{53} = -\frac{ScSrA_{14} m_2^2}{m_2^2 - B_{12}m_2 - B_{13}};$$

$$A_{54} = -\frac{ScSrA_{15}(m_1+m_2)^2}{(m_1+m_2)^2 - B_{12}(m_1+m_2) - B_{13}}; \quad A_{55} = -\frac{K_1 Sc}{B_{13}};$$

$$A_{46} = -(A_{47} + A_{48} + A_{49} + A_{50} + A_{51} + A_{52} + A_{53} + A_{54} + A_{55});$$

$$A_{47} = \frac{1}{-\mathrm{e}^{m_{13}} + \mathrm{e}^{m_{14}}}\big(1 - A_{48}\big(\mathrm{e}^{m_7} - \mathrm{e}^{m_{13}}\big) - A_{49}\big(\mathrm{e}^{m_8} - \mathrm{e}^{m_{13}}\big) - A_{50}\big(\mathrm{e}^{2m_1} - \mathrm{e}^{m_{13}}\big)$$
$$- A_{51}\big(\mathrm{e}^{2m_2} - \mathrm{e}^{m_{13}}\big) - A_{52}\big(\mathrm{e}^{m_1} - \mathrm{e}^{m_{13}}\big) - A_{53}\big(\mathrm{e}^{m_2} - \mathrm{e}^{m_{13}}\big)$$
$$- A_{54}\big(-\mathrm{e}^{m_{13}} + \mathrm{e}^{(m_1+m_2)}\big) - A_{55}\big(1 - \mathrm{e}^{m_{13}}\big)\big);$$

$$m_{15,16} = \frac{B_{12} \pm \sqrt{B_{12}^2 + 4B_{14}}}{2}; \quad B_{14} = \mathrm{i}H^2 Sc + \gamma Sc; \quad A_{58} = -\frac{ScSrA_{17} m_9^2}{m_9^2 - B_{12}m_9 - B_{14}};$$

$$A_{59} = -\frac{ScSrA_{18} m_{10}^2}{m_{10}^2 - B_{12}m_{10} - B_{14}}; \quad A_{60} = -\frac{ScSrA_{19}(m_1+m_3)^2}{(m_1+m_3)^2 - B_{12}(m_1+m_3) - B_{14}};$$

$$A_{61} = -\frac{ScSrA_{20}(m_1+m_4)^2}{(m_1+m_4)^2 - B_{12}(m_1+m_4) - B_{14}}; \quad A_{62} = -\frac{ScSrA_{21}(m_2+m_3)^2}{(m_2+m_3)^2 - B_{12}(m_2+m_3) - B_{14}};$$

$$A_{63} = -\frac{ScSrA_{22}(m_2+m_4)^2}{(m_2+m_4)^2 - B_{12}(m_2+m_4) - B_{14}}; \quad A_{64} = -\frac{ScSrA_{23} m_1^2}{m_1^2 - B_{12}m_1 - B_{14}};$$

$$A_{65} = -\frac{ScSrA_{24} m_2^2}{m_2^2 - B_{12}m_2 - B_{14}}; \quad A_{66} = -\frac{ScSrA_{25} m_3^2}{m_3^2 - B_{12}m_3 - B_{14}}; \quad A_{67} = -\frac{ScSrA_{26} m_4^2}{m_4^2 - B_{12}m_4 - B_{14}};$$

$$A_{56} = -(A_{57} + A_{58} + A_{59} + A_{60} + A_{61} + A_{62} + A_{63} + A_{64} + A_{65} + A_{66} + A_{67});$$

$$A_{57} = \frac{1}{-\mathrm{e}^{m_{15}} + \mathrm{e}^{m_{16}}}\big(A_{58}\big(\mathrm{e}^{m_{15}} - \mathrm{e}^{m_9}\big) + A_{59}\big(\mathrm{e}^{m_{15}} - \mathrm{e}^{m_{10}}\big) + A_{60}\big(\mathrm{e}^{m_{15}} - \mathrm{e}^{(m_1+m_3)}\big)$$
$$+ A_{61}\big(\mathrm{e}^{m_{15}} - \mathrm{e}^{(m_1+m_4)}\big) + A_{62}\big(\mathrm{e}^{m_{15}} - \mathrm{e}^{(m_2+m_3)}\big) + A_{63}\big(\mathrm{e}^{m_{15}} - \mathrm{e}^{(m_2+m_4)}\big)$$
$$+ A_{64}\big(\mathrm{e}^{m_{15}} - \mathrm{e}^{m_1}\big) + A_{65}\big(\mathrm{e}^{m_{15}} - \mathrm{e}^{m_2}\big) + A_{66}\big(\mathrm{e}^{m_{15}} - \mathrm{e}^{m_3}\big) + A_{67}\big(\mathrm{e}^{m_{15}} - \mathrm{e}^{m_4}\big)\big);$$

$$m_{17,18} = \frac{B_{12} \pm \sqrt{B_{12}^2 + 4B_{15}}}{2}; \quad B_{15} = 2\mathrm{i}H^2 Sc + \gamma Sc; \quad A_{70} = -\frac{ScSrA_{28} m_{11}^2}{m_{11}^2 - B_{12}m_{11} - B_{15}};$$

$$A_{71} = -\frac{ScSrA_{29} m_{12}^2}{m_{12}^2 - B_{12}m_{12} - B_{15}}; \quad A_{72} = -\frac{4ScSrm_3^2 A_{30}}{4m_3^2 - 2m_3 B_{12} - B_{15}};$$

$$A_{73} = -\frac{4ScSrm_4^2 A_{31}}{4m_4^2 - 2m_4 B_{12} - B_{15}}; \quad A_{74} = -\frac{ScSrA_{32}(m_3+m_4)^2}{(m_3+m_4)^2 - B_{12}(m_3+m_4) - B_{15}};$$

$$A_{75} = -\frac{ScSrA_{33}(m_1+m_3)^2}{(m_1+m_3)^2 - B_{12}(m_1+m_3) - B_{15}}; \quad A_{76} = -\frac{ScSrA_{34}(m_1+m_4)^2}{(m_1+m_4)^2 - B_{12}(m_1+m_4) - B_{15}};$$

$$A_{77} = -\frac{ScSrA_{35}(m_2+m_3)^2}{(m_2+m_3)^2 - B_{12}(m_2+m_3) - B_{15}}; \quad A_{78} = -\frac{ScSrA_{36}(m_2+m_4)^2}{(m_2+m_4)^2 - B_{12}(m_2+m_4) - B_{15}};$$
$$A_{79} = -\frac{ScSrA_{37}(m_1+m_5)^2}{(m_1+m_5)^2 - B_{12}(m_1+m_5) - B_{15}}; \quad A_{80} = -\frac{ScSrA_{38}(m_1+m_6)^2}{(m_1+m_6)^2 - B_{12}(m_1+m_6) - B_{15}};$$
$$A_{81} = -\frac{ScSrA_{39}(m_2+m_5)^2}{(m_2+m_5)^2 - B_{12}(m_2+m_5) - B_{15}}; \quad A_{82} = -\frac{ScSrA_{40}(m_2+m_6)^2}{(m_2+m_6)^2 - B_{12}(m_2+m_6) - B_{15}};$$
$$A_{83} = -\frac{ScSrA_{41}m_3^2}{m_3^2 - B_{12}m_3 - B_{15}}; \quad A_{84} = -\frac{ScSrA_{42}m_4^2}{m_4^2 - B_{12}m_4 - B_{15}};$$
$$A_{85} = -\frac{ScSrA_{43}m_5^2}{m_5^2 - B_{12}m_5 - B_{15}}; \quad A_{86} = -\frac{ScSrA_{44}m_6^2}{m_6^2 - B_{12}m_6 - B_{15}};$$
$$\begin{aligned} A_{68} = {} & -(A_{69} + A_{70} + A_{71} + A_{72} + A_{73} + A_{74} + A_{75} + A_{76} + A_{77} \\ & + A_{78} + A_{79} + A_{80} + A_{81} + A_{82} + A_{83} + A_{84} + A_{85} + A_{86}); \end{aligned}$$
$$\begin{aligned} A_{69} = {} & \frac{1}{\mathrm{e}^{m_{18}} - \mathrm{e}^{m_{17}}}\big(A_{70}\big(\mathrm{e}^{m_{17}} - \mathrm{e}^{m_{11}}\big) + A_{71}\big(\mathrm{e}^{m_{17}} - \mathrm{e}^{m_{12}}\big) + A_{72}\big(\mathrm{e}^{m_{17}} - \mathrm{e}^{2m_3}\big) \\ & + A_{73}\big(\mathrm{e}^{m_{17}} - \mathrm{e}^{2m_4}\big) + A_{74}\big(\mathrm{e}^{m_{17}} - \mathrm{e}^{(m_3+m_4)}\big) + A_{75}\big(\mathrm{e}^{m_{17}} - \mathrm{e}^{(m_1+m_3)}\big) \\ & + A_{76}\big(\mathrm{e}^{m_{17}} - \mathrm{e}^{(m_1+m_4)}\big) + A_{77}\big(\mathrm{e}^{m_{17}} - \mathrm{e}^{(m_2+m_3)}\big) + A_{78}\big(\mathrm{e}^{m_{17}} - \mathrm{e}^{(m_2+m_4)}\big) \\ & + A_{79}\big(\mathrm{e}^{m_{17}} - \mathrm{e}^{(m_1+m_5)}\big) + A_{80}\big(\mathrm{e}^{m_{17}} - \mathrm{e}^{(m_1+m_6)}\big) + A_{81}\big(\mathrm{e}^{m_{17}} - \mathrm{e}^{(m_2+m_5)}\big) \\ & + A_{82}\big(\mathrm{e}^{m_{17}} - \mathrm{e}^{(m_2+m_6)}\big) + A_{83}\big(\mathrm{e}^{m_{17}} - \mathrm{e}^{m_3}\big) + A_{84}\big(\mathrm{e}^{m_{17}} - \mathrm{e}^{m_4}\big) \\ & + A_{85}\big(\mathrm{e}^{m_{17}} - \mathrm{e}^{m_5}\big) + A_{86}\big(\mathrm{e}^{m_{17}} - \mathrm{e}^{m_6}\big)\big). \end{aligned}$$

References

1. M.H. Abolbashari, N. Freidoonimehr, F. Nazari, M.M. Rashidi, Analytical modeling of entropy generation for Casson nano-fluid flow induced by a stretching surface, *Adv. Powder Technol.*, **26**:542–552, 2015.
2. A.A. Afify, N.S. Elgazery, Lie group analysis for the effects of chemical reaction on MHD stagnation-point flow of heat and mass transfer towards a heated porous stretching sheet with suction or injection, *Nonlinear Anal. Model. Control*, **17**(1):1–15, 2012.
3. F. Ali, S. Nadeem Ahmad, I. Khan, M. Saqib, Magnetic field effect on blood flow of Casson fluid in axisymmetric cylindrical tube: A fractional model, *J. Magn. Magn. Mater.*, **423**:327–336, 2017.
4. H.A. Attia, M.E. Sayed-Ahmed, Transient MHD Couette flow of a Casson fluid between parallel with heat transfer, *Ital. J. Pure Appl. Math.*, **27**:19–38, 2010.
5. O.A. Beg, M.M. Rashidi, T.A. Beg, M. Asadi, Homotopy analysis of transient magneto-bio-fluid dynamics of micropolar squeeze film in a porous medium: A model for magneto-bio-rhelogical lubrication, *J. Mech. Med. Biol.*, **12**(3):1250051, 2012.
6. O.A. Beg, M.J. Uddin, M.M. Rashidi, N. Kavyani, Double-diffusive radiative magnetic mixed convective slip flow with Biot and Richardson number effects, *J. Eng. Thermophys.*, **23**(2):79–97, 2014.
7. A.R. Bestman, Pulsatile flow in heated porous channel, *Int. J. Heat Mass Transfer*, **25**:675–682, 1982.

8. C. Bridges, K.R. Rajagopal, Pulsatile flow of a chemically-reacting nonlinear fluid, *Comput. Math. Appl.*, **52**(6–7):1131–1144, 2006.
9. N. Casson, A flow equation for the pigment oil suspensions of the printing ink type, in C.C. Mill (Ed.), *Rheology of Disperse Systems*, Pergamon, New York, 1959, pp. 84–102.
10. N. Datta, D.C. Dalal, S.K. Mishra, Unsteady heat transfer to pulsatile flow of a dusty viscous incompressible fluid in a channel, *Int. J. Heat Mass Transfer*, **36**(7):1783–1788, 1993.
11. M. Hameed, S. Nadeem, Unstaedy MHD flow of a non-newtonian fluid on a porous plate, *J. Math. Anal. Appl.*, **325**(1):724–733, 2007.
12. T. Hayat, M. Mustafa, S. Asghar, Unsteady flow with heat and mass transfer of a third grade fluid over a stretching surface in the presence of chemical reaction, *Nonlinear Anal., Real World Appl.*, **11**(4):3186–3197, 2010.
13. T. Hayat, R. Sajjad, Z. Abbas, M. Sajjad, A.A. Hendi, Radiation effects on MHD flow of Maxwell fluid in a channel with porous medium, *Int. J. Heat Mass Transfer*, **54**(4):854–862, 2011.
14. T. Hayat, H. Yasmin, M. Al-Yami, Soret and Dufour effects in peristaltic transport of physiological fluids with chemical reaction: A mathematical analysis, *Comput. Fluids*, **89**:242–253, 2014.
15. H. Khan, M. Qayyum, O. Khan, M. Ali, Unsteady squeezing flow of Casson fluid with magnetohydrodynamic effect and passing through porous medium, *Math. Probl. Eng.*, **2016**:4293721, 2016.
16. F. Mabood, R.G.A. Rahman, G. Lorenzini, Effect of melting heat transfer and thermal radiation on Casson fluid flow in porous medium over moving surface with magnetohydrodynamics, *J. Eng. Thermophys.*, **25**(4):536–547, 2016.
17. O.D. Makinde, Free convection flow with thermal radiation and mass transfer past a moving vertical porous plate, *Int. Commun. Heat Mass*, **32**:1411–1419, 2005.
18. T. Malathy, S. Srinivas, Pulsating flow of a hydromagnetic fluid between permeable beds, *Int. Commun. Heat Mass*, **35**(5):681–688, 2008.
19. T. Malathy, S. Srinivas, A.S. Reddy, Chemical reaction and thermal radiation effects on MHD pulsatile flow of an Oldroyd-B fluid in a porous medium with slip and convective boundary conditions, *J. Porous Media*, **20**(4):287–301, 2017.
20. J.C. Misra, G.C. Shit, S. Chandra, P.K. Kundu, Hydromagnetic flow and heat transfer of a second-grade viscoelastic fluid in a channel with oscillatory stretching walls: Application to the dynamics of blood flow, *J. Eng. Math.*, **69**(1):91–100, 2011.
21. S. Mukhopadhyay, K. Vajravelu, Diffusion of chemically reactive species in Casson fluid flow over an unsteady permeable stretching surface, *J. Hydrodyn.*, **25**(4):591–598, 2013.
22. M. Mustafa, T. Hayat, I. Pop, A. Aziz, Unsteady boundary layer flow of a Casson fluid due to an impulsively started moving flat plate, *Heat Transfer Asian Res.*, **40**:563–576, 2011.
23. D. Mythili, R. Sivaraj, Influence of higher order chemical reaction and non-uniform heat source/sink on Casson fluid flow over a vertical cone and flat plate, *J. Mol. Liq.*, **216**:466–475, 2016.
24. D. Mythili, R. Sivaraj, M.M. Rashidi, Heat generating/absorbing and chemically reacting Casson fluid flow over a vertical cone and flat plate saturated with non-Darcy porous medium, *Int. J. Numer. Methods Heat Fluid Flow*, **27**(1):156–173, 2017.

25. S. Nadeem, R. Ul Haq, C. Lee, MHD flow of a Casson fluid over an exponentially shrinking sheet, *Sci. Iran.*, **19**(6):1550–1553, 2012.

26. S. Nadeem, R. Ul-Haq, N.S. Akbar, Z.H. Khan, MHD three-dimensional Casson fluid flow past a porous linearly stretching sheet, *Alexandria Eng. J.*, **52**(4):577–582, 2013.

27. G. Palani, I.A. Abbas, Free convection MHD flow with thermal radiation from an impulsively-started vertical plate, *Nonlinear Anal. Model. Control*, **14**(1):73–84, 2009.

28. K.V. Prasad, P. Mallikarjun, H. Vaidya, Mixed convective fully developed flow in a vertical channel in the presence of thermal radiation and viscous dissipation, *Int. J. Appl. Mech. Eng.*, **22**(1):123–144, 2017.

29. K.V. Prasad, K. Vajravelu, I.S. Shivakumara, H. Vaidya, N.Z. Basha, Flow and heat transfer of a Casson nanofluid over a nonlinear stretching sheet, *J. Nanofluids*, **5**:743–752, 2016.

30. K.V. Prasad, K. Vajravelu, H. Vaidya, MHD Casson nanofluid flow and heat transfer at a stretchingsheet with variable thickness, *J. Nanofluids*, **5**:423–435, 2016.

31. K.V. Prasad, K. Vajravelu, H. Vaidya, N.Z. Basha, V. Umesh, Thermal and species concentration of MHD Casson fluid at a vertical sheet in the presence variable fluid properties, *Ain Shams Eng. J.*, 2017 (in press), `https://doi.org/10.1016/j.asej.2016.08.017`.

32. B. Punnamchandar, T.K.V. Iyengar, Pulsating flow of an incompressible micropolar fluid between permeable beds, *Nonlinear Anal. Model. Control*, **18**(4):399–411, 2013.

33. G. Radhakrishnamacharya, M.K. Maiti, Heat transfer to pulsatile flow in a porous channel, *Int. J. Heat Mass Transfer*, **20**(2):171–173, 1977.

34. M.M. Rashidi, E. Momoniat, B. Rostami, Analytic approximate solutions for MHD boundary-layer viscoelastic fluid flow over continuously moving stretching surface by homotopy analysis method with two auxiliary parameters, *J. Appl. Math.*, **2012**:780415, 2012.

35. A.S. Reddy, S. Srinivas, T.R. Ramamohan, Analysis of heat and chemical reaction on an asymmetric laminar flow between slowly expanding or contracting walls, *Heat Transfer Asian Res.*, **42**(5):422–443, 2013.

36. D.S. Sankar, A two-fluid model for pulsatile flow in catheterized blood vessels, *Int. J. Non-Linear Mech.*, **44**:337–351, 2009.

37. S.A. Shehzad, T. Hayat, A. Alsaedi, M.A. Meraj, On a magnetohydrodynamic flow of the Casson fluid with partial slip and thermal radiation, *J. Appl. Mech. Tech. Phys.*, **57**(5):916–924, 2016.

38. G.C. Shit, M. Roy, Pulsatile flow and heat transfer of magneto-micropolar fluid through a stenosed artery under the influence of body acceleration, *J. Mech. Med. Biol.*, **11**(3):643–661, 2011.

39. A. Sinha, G.C. Shit, Electromagnetohydrodynamic flow of blood and heat transfer in a capillary with thermal radiation, *J. Magn. Magn. Mater.*, **378**:143–151, 2015.

40. R. Sivaraj, A.J. Benazir, Unsteady magnetohydrodynamic mixed convective oscillatory flow of Casson fluid in a porous asymmetric wavy channel, *Special Topics & Reviews in Porous Media: An International Journal*, **6**(3):267–281, 2015.

41. S. Srinivas, T. Malathy, A.S. Reddy, A note on thermal-diffusion and chemical reaction effects on MHD pulsating flow in a porous channel with slip and convective boundary conditions, *J. King Saud Univ.*, **28**(2):213–221, 2016.

42. S. Srinivas, T. Malathy, P.L. Sachdev, On pulsatile hydromagnetic flow of an Oldroyd fluid with heat transfer, *Eng. Trans.*, **55**(1):79–94, 2007.

43. S. Srinivas, A.K. Shukla, T.R. Ramamohan, A.S. Reddy, Influence of thermal radiation on unsteady flow over an expanding or contracting cylinder with thermal-diffusion and diffusion-thermo effects, *J. Aerosp. Eng.*, **28**(5):04014134, 2015.

44. K. Vajravelu, K.V. Prasad, N.S. Prasanna Rao, Diffusion of a chemically reactive species of a power-law fluid past a stretching surface, *Comput. Math. Appl.*, **62**(1):93–108, 2011.

45. K. Vajravelu, K.V. Prasad, H. Vaidya, N.Z. Basha, Ch.O. Ng, Mixed convective flow of a Casson fluid over a vertical stretching sheet, *Int. J. Appl. Comput. Math.*, **3**(3):1619–1638, 2017.

46. K. Vajravelu, K. Ramesh, S. Sreenadh, P.V. Arunachalam, Pulsatile flow between permeable beds, *Int. J. Non-Linear Mech.*, **38**:999–1005, 2003.

47. C.Y. Wang, Pulsatile flow in a porous channel, *J. Appl. Mech.*, **38**(2):553–555, 1971.